https://doi.org/10.20965/jaciii.2011.p0980

Paper:

Decomposition of Limb Movement Based on Muscular Coordination During Human Running

Taiki Iimura, Keita Inoue, Hang T. T. Pham, Hiroaki Hirai, and Fumio Miyazaki

Graduate School of Engineering Science, Osaka University
1-3 Machikaneyama-cho, Toyonaka, Osaka 560-8531
E-mail: {iimura@robotics., inoue@robotics., phamhangtt@robotics., hirai@, miyazaki@}me.es.osaka-u.ac.jp

[Received March 1, 2011; accepted May 28, 2011]

The study of decomposing movement into units of motor function is evolving in neuroscience. Meanwhile, in robotics, there is a problem with redundant Degrees Of Freedom (DOF) in the motor control of human-like robots. We attempt to achieve fewer-DOF control of a human-like musculoskeletal robot by using our knowledge of the units of motor function. In this paper, we introduce "the agonist-antagonist muscle pairs (A-A) ratio" and "A-A activity," which are defined by using ElectroMyoGraphic (EMG) data and which describe the coordination between the agonist and antagonist muscles. Human running is decomposed into two units of motor function from the point of view of muscle coordination using Principal Component Analysis (PCA) of these biological signals. The kinematic meanings of the extracted patterns of muscle coordination are visualized by human-like musculoskeletal leg robot.

Keywords: EMG, human running, motor primitive, principal component analysis, muscular coordination

1. Introduction

The problem of redundant degrees of freedom in the human body is known as Bernstein's problem. N. A. Bernstein, a Russian physiologist, attempted to solve the problem by explaining that a human flexibly adjusts the redundant degrees of freedom in coordinated motion for any purpose [1]. However, a clear description for this ill-posed problem has not yet been obtained. In neuroscience, there is an enormous amount of research on decomposing movement into units of motor function, which is said to be important for solving Bernstein's problem of redundant degrees of freedom. There are a potent hypothesis about the units of motor function; the muscle-synergy hypothesis [1–4]. It regards the Central Nervous System's (CNS's) commands to muscle groups as the units of motor function. It then combines the units of motor function of CNS to achieve movement.

As observed above, the study of decomposing movement into units of motor function is evolving, but its applications to robotics have not been deeply investigated yet. The present robot driven by DC servo motors is operated by position servo control. As the servo stiffness is adjusted as high as possible, it is difficult for the robot to modulate the joint stiffness in response to externally imposed disturbances. In contrast, the musculoskeletal robot can be designed based on biological motor control, which makes it possible to control its end-point stiffness intentionally. However, there is also a problem with redundant degrees of freedom in the human-like musculoskeletal robot's body or the Bernstein's problem. This problem makes it difficult to decide the appropriate motor commands because the inverse dynamics problem for such robots is underspecified. The application of the decomposition concept of a redundant muscle activity into a few units of motor function enables to describe the muscle activities with the dimension enough for motor control, which is anticipated to make an easier control of a redundant-DOF robot. In this paper, we extract units of motor function from muscle space based on the coordination of agonist-antagonist muscle pairs. We then visualize the kinematic meanings of these units by the musculoskeletal leg robot. The robot is used as a tool for demonstrating our theory of muscular coordination.

In a human's daily movement, the locomotion of the body is important. As a means of locomotion, the movement of a leg can be classified into two main movements, walking and running. Cappellini et al. extracted five principal components as basis vectors in the muscle space by using Principal Component Analysis (PCA) on a data set of 32 muscles' ElectroMyoGraphy (EMG) in human walking and running [2]. Ivanenko et al. also analyzed the joint angles by the same statistical method and demonstrated a correspondence relation between the extracted principal components and the toe's motions in a polar coordinate system based on the hip joint [5]. They discussed the motor primitives in the muscle space and joint space independently, but they did not demonstrate the relation between their spaces. In our previous study, we introduced the concept of "the agonist-antagonist muscle pairs (A-A) ratio," defined as the ratio of EMGs for the antagonist and agonist muscles, and decomposed human walking into two motor primitives having kinematic functions by using PCA for the A-A ratios [6]. Transferring two units of motor function extracted from the A-A ratios in human walking into the musculoskeletal robot revealed that each unit of motor function was concerned with the argument and moving radius of the toe in a polar coordinate system based on the hip joint. The A-A ratio thus can be said to contribute to the joint angles.

In this paper, human running, the other main means of locomotion, is investigated. We propose two concept, the "A-A ratio" and "A-A activity," which represent the coordination of agonist-antagonist muscle pairs. The A-A ratio is defined as the ratio of an extensor muscle's EMG to the sum of the agonist and antagonist muscles' EMG, and it is considered to describe the degree of extension of the joints over a 0 to 1 range. A-A activity is defined as the sum of the EMGs for agonist and antagonist muscles, and it can be treated as a parameter to relate to the degree of stiffness of the joints. Each of these parameters based on the EMG signals during human running is decomposed into two principal components. In this paper, we analyze the Principal Component (PC) vectors of two parameters, A-A ratio and A-A activity. We then demonstrate that (1) human running can be decomposed into two patterns of muscle coordinations associated with kinematics and (2) we also develop a new method of controlling a musculoskeletal robot using patterns of muscle coordination.

This paper is organized as follows. Section 2 provides the definitions of the A-A ratio and A-A activity, and explains the PCA technique. Section 3 discusses the decomposition of human running into patterns of muscle coordination. We also explain the identification of the kinematic meanings of extracted patterns by using the musculoskeletal leg robot. Finally, Section 4 summarizes our results.

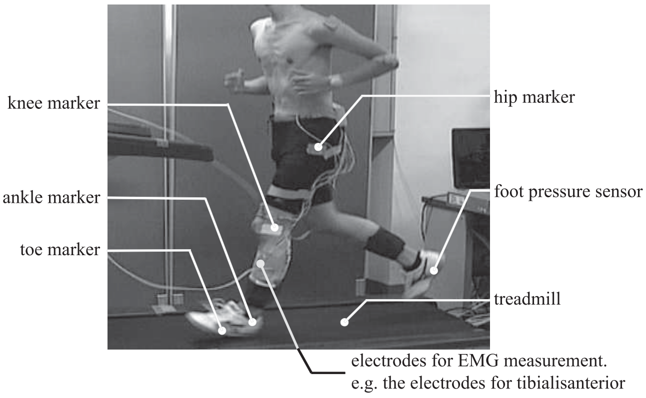

Fig. 1. Motion measurement of human running.

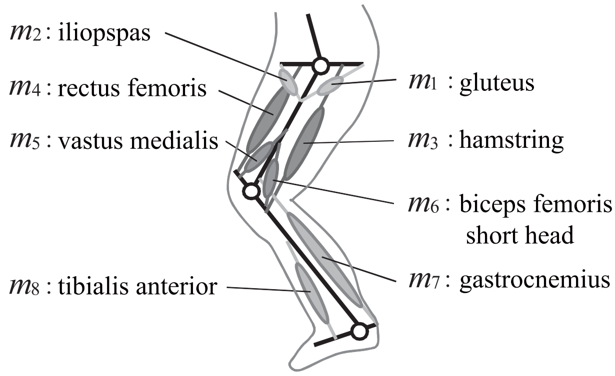

Fig. 2. Musculoskeletal model of human lower limb.

2. Motion Measurement

2.1. Experiment Setup

Three healthy subjects, A (male, 23 years old, 1.75 m, 60.4 kg, right-legged), B (male, 23 years old, 1.70 m, 54.0 kg, right-legged), and C (male, 23 years old, 1.74 m, 60.0 kg, right-legged), volunteered for the experiment. Approval for this study was provided by the Ethics Committee of Osaka University, Graduate School of Engineering Science, and informed consent was obtained from these subjects. **Fig. 1** depicts motion measurement during treadmill running. Each subject ran on the treadmill (SportsArt Fitness T650m) at different speeds (7, 9, 11, 13 km/h) for 30 seconds and kinematic data (hip, knee and ankle joint positions) were measured using a motion-capture system, QuickMAG System III (OKK, Inc.), at 60 Hz. The lower limb was modeled as a simple three-link system in the sagittal plane (**Fig. 2**). The surface EMG activities of eight muscles of the left leg were recorded using a multitelemeter system, WEB-5000 (Nihon Koden), at 1000 Hz. This system sends EMG data to a personal computer after band-pass filtering (0.03 to 450 Hz), antihum filtering (around 60 Hz), and amplificating ($\times$ 2000) process. The chosen eight muscles are as follows: gluteus (m_1), iliopspas (m_2), hamstring (except biceps femoris short head) (m_3), rectus femoris (m_4), vastus medialis (m_5), biceps femoris short head (m_6), gastrocnemius (m_7) and tibialis anterior (m_8) (**Fig. 2**). These mono- and bi-articular muscles are the major muscles relevant to hip, knee and ankle joint movements [7]. The skin areas were cleaned with alcohol and abraded to reduce skin resistance ($<$ 10 kΩ). The interelectrode distance was 2 cm. A run cycle was defined with respect to the left leg movement, beginning with left-heel contact with the ground and ending with next left-heel contact. The foot pressure was recorded by F-SCAN MOBILE (Nitta) at 500 Hz to detect the time of heel contact. Each subject wore foot-pressure sensors over their shoes. The EMG measurement device, the foot pressure measurement device, and the motion-capture system were synchronized.

2.2. Data Analysis

A data analysis was performed after the following preparations for raw EMG data: band-pass filtering (20 to 450 Hz) (a typical procedure in EMG analysis [8]), full-wave rectification, smoothing, and normalization to Maximum Voluntary Contraction (%MVC). The muscles for experiment are expressed as m_i $(i = 1, \dots, 8)$ (**Fig. 2**). These %MVC data were averaged by using 29–36 run cycles.

In this study, we focus on the coordination between the agonist and antagonist muscles, defining the A-A ratio

Table 1. Definition of the agonist-antagonist muscle-pair ratio.

Pair label	Target muscles	Movement function
r_1	$m_1/(m_1+m_2)$	Hip extension
r_2	$m_3/(m_3+m_4)$	Hip extension and Knee flexion
r_3	$m_5/(m_5+m_6)$	Knee extension
r_4	$m_7/(m_7+m_8)$	Ankle extension
r_5	$m_1/(m_1+m_4)$	Hip extension
r_6	$m_3/(m_2+m_3)$	Hip extension (and Knee flexion)
r_7	$m_5/(m_3+m_5)$	Knee extension
r_8	$m_4/(m_4+m_6)$	Knee extension (and hip flexion)
r_9	$m_5/(m_5+m_7)$	Knee extension

Table 2. Definition of the agonist-antagonist muscle-pair activity.

Pair label	Target muscles	Physical property
a_1	m_1+m_2	Hip joint stiffness
a_2	m_3+m_4	Hip and Knee joint stiffness
a_3	m_5+m_6	Knee joint stiffness
a_4	m_7+m_8	Ankle joint stiffness
a_5	m_1+m_4	Hip joint stiffness
a_6	m_2+m_3	Hip joint stiffness
a_7	m_3+m_5	Knee joint stiffness
a_8	m_4+m_6	Knee joint stiffness
a_9	m_5+m_7	Knee joint stiffness

Table 3. Run cycle T [sec].

Subject	7 km/h	9 km/h	11 km/h	13 km/h
A	0.694	0.673	0.667	0.647
B	0.760	0.707	0.706	0.634
C	0.780	0.746	0.707	0.687

$r_i(t)$ $(i=1,\ldots,9)$ and A-A activity $a_i(t)$ $(i=1,\ldots,9)$ in **Tables 1** and **2**. These definitions enable treating two parameters: one contributing to the joint angle and the other contributing to joint stiffness. For example, when a hip joint is extending, the extensor muscle's EMG (m_1) increases and the flexor muscle's EMG (m_2) decreases, resulting in an increase in the A-A ratio r_1. For this reason, the A-A ratio r_1 can be said to contribute to the hip-joint angle. Meanwhile, for instance, when the hip joint stiffness is increasing, both m_1 and m_2 are increasing, resulting in an increase in A-A activity a_1. For this reason, A-A activity a_1 can be said to contribute to the hip joint stiffness. From here on, we analyze human running by using these two parameters based on the EMG signals.

The A-A ratio data set for run cycle T (**Table 3**) is expressed as $\boldsymbol{R}=\{r_j(t_i)\}$ (a $p\times q$ matrix, where $r_j(t_i)$ is the j-th A-A ratio at time t_i, p is the number of time-points during a run cycle, and q is the number of the pair labels of A-A ratios). In this experiment, $p=634\sim 780$ and $q=9$. Note that the number p varies according to the run speed because of the varying run cycle. Matrix $\boldsymbol{R}$ is expressed as follows.

$$\boldsymbol{R}=\begin{bmatrix} r_1(t_1) & r_2(t_1) & \cdots & r_9(t_1) \\ r_1(t_2) & r_2(t_2) & \cdots & r_9(t_2) \\ \vdots & \vdots & \ddots & \vdots \\ r_1(t_p) & r_2(t_p) & \cdots & r_9(t_p) \end{bmatrix} \quad . \ . \ . \ (1)$$

The A-A activity data set $\boldsymbol{A}=\{a_j(t_i)\}$ is expressed as the following in the same way.

$$\boldsymbol{A}=\begin{bmatrix} a_1(t_1) & a_2(t_1) & \cdots & a_9(t_1) \\ a_1(t_2) & a_2(t_2) & \cdots & a_9(t_2) \\ \vdots & \vdots & \ddots & \vdots \\ a_1(t_p) & a_2(t_p) & \cdots & a_9(t_p) \end{bmatrix} \quad . \ . \ (2)$$

Applying PCA to the A-A ratio data set $\boldsymbol{R}$ or A-A activity data set $\boldsymbol{A}$ results in the linear combinations:

$$\begin{cases} \mathrm{diag}[\boldsymbol{\sigma}_r]^{-1}\left(\boldsymbol{r}(t)-\bar{\boldsymbol{r}}\right) = \sum_{i=1}^{9} w_{ri}(t)\boldsymbol{p}_{ri} \\ \mathrm{diag}[\boldsymbol{\sigma}_a]^{-1}\left(\boldsymbol{a}(t)-\bar{\boldsymbol{a}}\right) = \sum_{i=1}^{9} w_{ai}(t)\boldsymbol{p}_{ai} \end{cases} \quad (3)$$

where $\boldsymbol{r}(t)=[r_1(t),r_2(t),\ldots,r_9(t)]^T$ is an A-A ratio data set vector, $\boldsymbol{a}(t)=[a_1(t),a_2(t),\ldots,a_9(t)]^T$ is an A-A activity data set vector, $\mathrm{diag}[\boldsymbol{\sigma}_r]$ is a 9×9 diagonal matrix with r_i's standard deviation σ_{ri} in the i-th row and i-th column, $\mathrm{diag}[\boldsymbol{\sigma}_a]$ is a 9×9 diagonal matrix with a_i's standard deviation σ_{ai} in the i-th row and i-th column, $\bar{\boldsymbol{r}}$ and $\bar{\boldsymbol{a}}$ are the mean vectors, $w_{ri}(t)$ and $w_{ai}(t)$ are the i-th Principal Component (PC) scores, and $\boldsymbol{p}_{ri}=[p_{ri1},p_{ri2},\ldots,p_{ri9}]^T$ or $\boldsymbol{p}_{ai}=[p_{ai1},p_{ai2},\ldots,p_{ai9}]^T$ is the i-th 9-dimensional PC vector of the A-A ratio or A-A activity.

3. Decomposition of Human Running

The PCA technique decomposes the A-A ratio and the A-A activity data set into linear combinations (Eq. (3)). The PC vectors of the A-A ratio $\boldsymbol{p}_{ri}$ and A-A activity $\boldsymbol{p}_{ai}$ are the units of motor function that describe the balance among the eight muscles. This concept supports the muscle-synergy hypothesis, which regards the CNS's commands to muscle groups as the units of motor function [1]. In all cases, the cumulative contribution rates up to the second principal component are more than 95%. **Tables 4** and **5** present the contribution rates of two PCs of A-A ratio and A-A activity, respectively. This indicates that two principal components can describe the most of eight muscle activities.

3.1. A-A Ratio and the Musculoskeletal Leg Robot

There is little difference in each pattern of the first or second PC vectors at all running speeds, so we treat the first and second PC vectors as "muscle coordination 1" and "muscle coordination 2," respectively. **Fig. 3** depicts the first and second PC vectors of the A-A ratio (muscle coordination 1 and 2) for the three subjects using a boxplot in which the horizontal axis is the number of the

Table 4. The contribution rates [%] of first and second PCs of A-A ratio.

Subject	7 km/h		9 km/h		11 km/h		13 km/h	
	PC1	PC2	PC1	PC2	PC1	PC2	PC1	PC2
A	67.4	29.1	60.5	34.5	60.9	35.4	57.3	36.0
B	52.8	44.2	65.2	33.7	61.3	37.6	61.2	37.7
C	63.5	35.6	62.5	36.4	65.0	34.0	65.4	33.9

Table 5. The contribution rates [%] of first and second PCs of A-A activity.

Subject	7 km/h		9 km/h		11 km/h		13 km/h	
	PC1	PC2	PC1	PC2	PC1	PC2	PC1	PC2
A	94.4	5.20	96.2	3.51	96.2	3.53	96.0	3.81
B	87.8	11.4	89.2	10.1	87.4	11.9	71.5	23.5
C	59.6	34.1	64.9	29.0	73.7	23.3	75.4	22.6

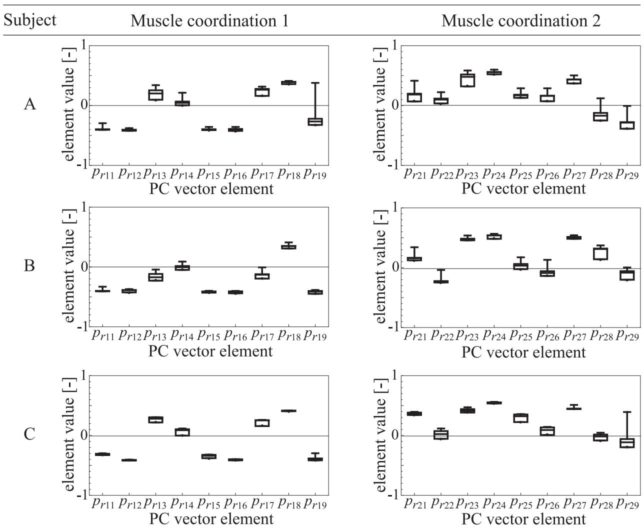

Fig. 3. Two patterns of PC vectors of A-A ratio.

PC vector elements; the vertical axis is the PC vector elements' value; the middle of each box is the sample average of the PC vector elements at all running speeds; the length of each box is twice the standard deviation of different running speeds; the top (bottom) of the line segment extending from each box is the maximum (minimum) values of the PC vector elements at all running speeds; and the dividing line in each box is the median value of the PC vector elements at all running speeds. The fact that all of the boxes are relatively short compared with the norm for the PC vector (the norm is 1) indicates that the standard deviation of the PC vector's element at different run speeds is small. This implies that the patterns of muscle coordination do not depend on the run speed (7, 9, 11, 13 km/h). Additionally, the difference in the patterns of muscle coordination among the three subjects was small. **Table 6** presents the cosine values of the angle between each subject's PC vectors of A-A ratios averaged at all run speeds. In all cases, most cosine values are close to 1.0, which indicates that there is little difference among the three subjects' patterns of muscle coordination.

Table 6. Cosine values of the angle between the different subject's PC vectors of A-A ratios.

Muscle coordination 1			Muscle coordination 2		
Subject A, B	B, C	A, C	Subject A, B	B, C	A, C
0.81	0.84	0.96	0.81	0.86	0.94

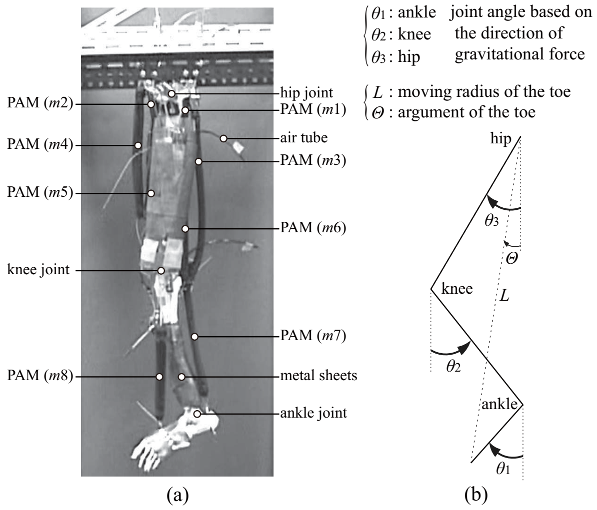

Fig. 4. The musculoskeletal leg robot.

Muscle coordinations 1 and 2 ($\boldsymbol{p}_{r1}$ and $\boldsymbol{p}_{r2}$), extracted from the A-A ratios, contribute to the joint angles, and seem to contain the kinematic meanings independently to each other. To confirm the kinematic meaning of these two patterns of muscle coordination in human running, we transferred these patterns to our human-like musculoskeletal leg robot. **Fig. 4(a)** presents the human-like musculoskeletal leg robot. The robot consists of a skeletal model (Avice, Inc.) and eight Pneumatic Artificial Muscles (PAMs) (Kanda Tsushin Kogyo Co., Ltd.) corresponding to the examined muscles, as illustrated in **Fig. 2**. The robot's body parameters (segment mass, moment of inertia) are reconstructed from human [9, 10] by attaching metal sheets to the robot. The muscle-attaching locations were decided by referring to human muscles (**Fig. 2**). The robot has three degrees of freedom, with the rotation of the hip, knee, and ankle joints in the sagittal plane. Air pressure supplied to the PAM is controlled by voltage commands from the computer sent to an air-pressure-control device (Hitachi Medical Corp.) that powers the pressure according to the voltage changes via a proportional electromagnetic valve. The air-pressure command was determined by two parameters; the A-A ratio κ and the A-A activity μ. These two parameters are defined as

$$\left\{ \begin{array}{lcl} \kappa & = & \dfrac{p_1}{p_1+p_2} \\ \mu & = & p_1+p_2 \end{array} \right. \quad . \; . \; . \; . \; . \; . \; . \; . \; . \; . \quad (4)$$

where p_1 and p_2 are air-pressure commands to the agonist-antagonist muscle pairs. Solving Eq. (4) for parameters p_1 and p_2 yields the following.

$$\left\{ \begin{array}{lcl} p_1 & = & \kappa\mu \\ p_2 & = & (1-\kappa)\mu \end{array} \right. \quad . \; . \; . \; . \; . \; . \; . \; . \; . \quad (5)$$

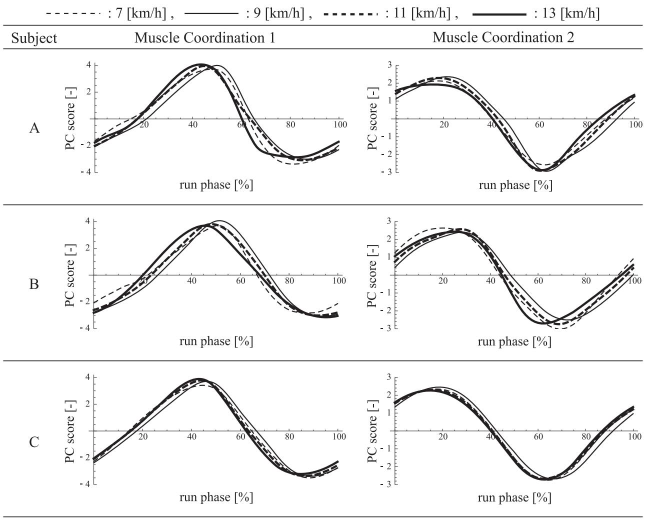

Fig. 5. Two PC scores of the A-A ratio in the case of subject A, B and C.

Because $\kappa \in [0,1]$, the A-A activity μ is the maximal air-pressure command to the PAMs. In our experiments, the A-A activity μ of all PAMs was fixed at an experimentally determined constant ($\mu = 500$ kPa) to refer to the kinematic meaning of the PC vectors of A-A ratios. To transfer muscle coordinations 1 and 2 of the A-A ratios ($\boldsymbol{p}_{r1}$, $\boldsymbol{p}_{r2}$) into the leg robot, we introduce two PCs of the A-A ratios of the robot, $\boldsymbol{K}_1$ and $\boldsymbol{K}_2$. These parameters correspond to the first and second PCs of the human A-A ratios. These are then determined using the first and second PC vectors of the human A-A ratio as follows, according to Eq. (3):

$$\begin{cases} \boldsymbol{K}_1(t) = W_1(t)\mathrm{diag}[\boldsymbol{\sigma}_r]\boldsymbol{p}_{r1} + \bar{\boldsymbol{r}} \\ \boldsymbol{K}_2(t) = W_2(t)\mathrm{diag}[\boldsymbol{\sigma}_r]\boldsymbol{p}_{r2} + \bar{\boldsymbol{r}} \end{cases} \quad \ldots\ldots \quad (6)$$

$\boldsymbol{K}_i\,(i = 1,2)$ consists of the A-A ratios κ of artificial muscle pairs. Because the parameters $\kappa(t)$ of muscle pairs can be determined in Eq. (6), it is possible to decide the air-pressure commands in Eq. (5). $W_1(t)$ or $W_2(t)$ is a parameter that varies the size of the patterns of muscle coordination with the neutral pattern $\bar{\boldsymbol{r}}$ as a basis, and it corresponds to the PC score ($w_1(t)$ or $w_2(t)$) of the human A-A ratio. In this experiment, so as to visualize what is meant by the size of each PC score $w_{ri}(t)$ and how it contributes to each PC vectors $\boldsymbol{p}_{ri}$, $W_1(t)$ or $W_2(t)$ are changed linearly from -4.0 to 4.0 or from -3.0 to 3.0 in 50 seconds so as to cover the range of $w_1(t)$ or $w_2(t)$ (**Fig. 5**). **Fig. 6** shows the patterns of $W_1(t)$ and $W_2(t)$ given to the robot. (Note that $W_i(t)$ is not the same as $w_i(t)$.) The proportional changes in the PC vector elements enable the robot to achieve motion in a unique direction while retaining the pattern of muscle coordination. **Fig. 7** illustrates the leg robot's movements generated by the first or second pattern of muscle coordination in the case of subject C at 7 km/h. As seen in **Fig. 7**, based on a hip joint, muscle coordination 1 (the first PC vector of A-A ratios) seems to create a rotary motion of the toe's position, and muscle coordination 2 (the second PC vector of A-A ratios) seems to drive the toe's position closer to or away from the hip joint. The same results were obtained for different subjects at different running speeds. This result implies that human running is described by a combination of units of motor function that contribute to the argument Θ and the moving radius L of a toe, based on the hip joint (**Fig. 4(b)**).

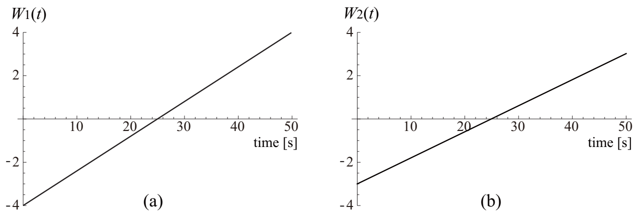

Fig. 6. The robot's PC scores of the A-A ratio, (a) $W_1(t)$, (b) $W_2(t)$.

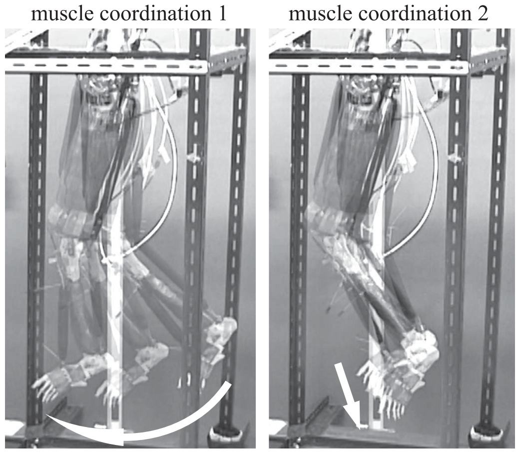

Fig. 7. Two patterned muscular coordinations of the musculoskeletal leg robot.

Ivanenko et al. achieved a similar result, although the analysis was performed in the joint space [5]. They decomposed locomotion into two principal components by using the joint angles $[\theta_1, \theta_2, \theta_3]^T$, based on the direction of gravitational force (**Fig. 4(b)**). According to their study, we analyzed the joint-angle space $[\theta_1, \theta_2, \theta_3]^T$ based on the direction of gravitational force using PCA. $\boldsymbol{\theta} = [\theta_1, \theta_2, \theta_3]^T$ can be expressed as follows:

$$\boldsymbol{\theta} = \sum_{i=1}^{3} w_{\theta i}(t)\boldsymbol{p}_{\theta i} + \bar{\boldsymbol{\theta}} \quad \ldots\ldots\ldots\ldots \quad (7)$$

where $w_{\theta i}(t)$ is i-th PC score, $\boldsymbol{p}_{\theta i} = [p_{\theta i1}, p_{\theta i2}, p_{\theta i3}]^T$ is the i-th PC vector, and $\bar{\boldsymbol{\theta}} = [\bar{\theta}_1, \bar{\theta}_2, \bar{\theta}_3]$ is the mean vector. **Fig. 8** depicts the result of simulation for two principal components in the case of subject C at 7 km/h as follows:

$$\boldsymbol{\theta}(t) = \begin{cases} w_{\theta 1}(t)\boldsymbol{p}_{\theta 1} + \bar{\boldsymbol{\theta}} \\ w_{\theta 2}(t)\boldsymbol{p}_{\theta 2} + \bar{\boldsymbol{\theta}} \end{cases} \quad \ldots\ldots\ldots \quad (8)$$

It seems that the motions of the musculoskeletal leg robot (**Fig. 7**) correspond to these kinematic results (**Fig. 8**). The same results were obtained for different subjects at

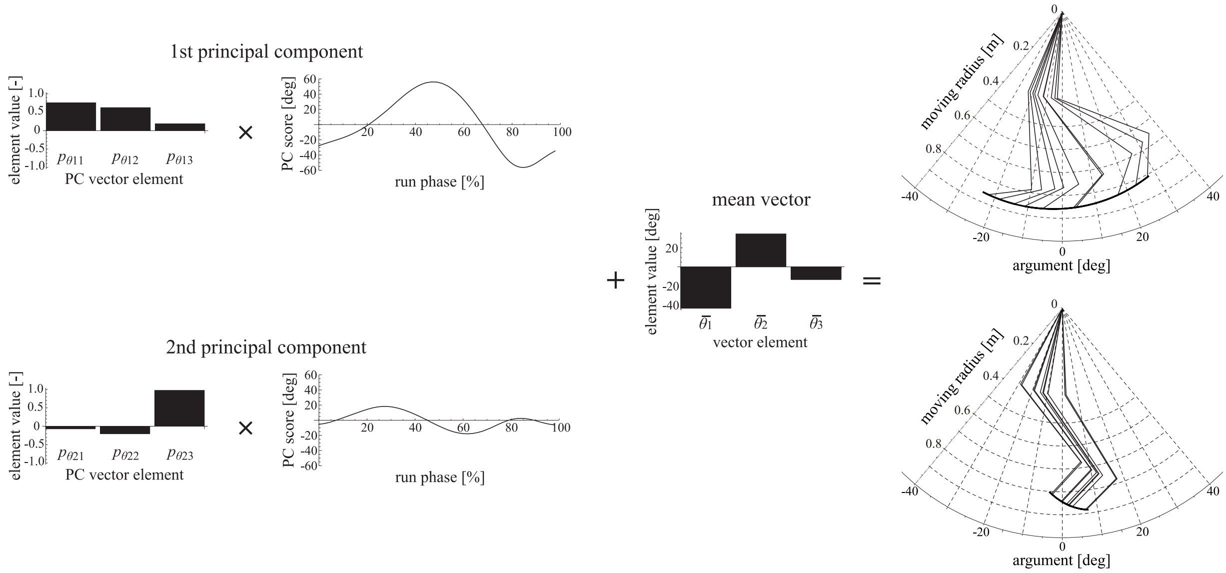

Fig. 8. Simulation for two principal components extracted from the joint angles.

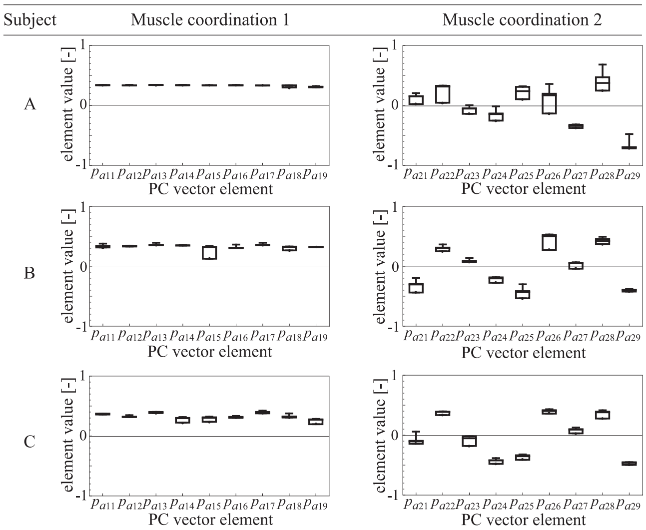

Fig. 9. Two patterns of PC vectors of A-A activity.

different running speeds.

So far we have considered the reduction of the muscle space's size and the meaning of the extracted motor primitives. These results are valid even if the size of the motor command space for musculoskeletal robot is huge relative to that for the robot driven by DC servo motors. As just described, the proposed method is useful for solving the ill-posed problem, or Bernstein's problem.

3.2. A-A Activity

The first PC vectors of the activity (muscle coordination 1 of the A-A activity) are similar for different subjects or different running speeds because of their high contribution ratio (subject A: 94.4–96.2%, subject B: 71.5–89.2%, subject C: 59.6–75.4%). Therefore, the contribution ratio of the second principal components is fatally low, and the second PC vectors (muscle coordination 2 of the A-A activity) are a little different for all running speeds of subject A while these similar for all running speeds of subject B or C (**Fig. 9**). **Table 7** lists the results of the same calculation as **Table 6** for the PC vectors of the A-A activities. Muscle coordination 1 did not differ among subjects A, B, and C, while muscle coordination 2 of subject A differed from that of the other subjects. This result indicates that one subject (subject A) may control joint stiffness by using only one pattern of muscle coordination, while the others (subjects B and C) may use another pattern of muscle coordination.

Table 7. Cosine values of the angle between the different subject's PC vectors of A-A activities.

Muscle coordination 1			Muscle coordination 2		
Subject A, B	B, C	A, C	Subject A, B	B, C	A, C
1.00	0.99	0.99	0.49	0.92	0.59

4. Conclusion

In this study, we introduced the A-A ratio and A-A activity, which describe the coordination of agonist-antagonist muscle pairs, and we discussed the decomposition of human running into units of motor function based on knowledge from neuroscience. Two units of motor function extracted by using PCA for the A-A ratio and A-A activity are expressed by PC vectors, which are time-invariant patterns of a muscle group's coordination, and by time-varying PC scores, which change the degrees of these two patterns' contribution to the movement. In this paper, we focused on the PC vectors. The result of transferring the patterns of muscle coordination (PC vectors) extracted from the A-A ratios into a pneumatically driven musculoskeletal leg robot implies that these patterns of muscle coordination contribute to the argument and the moving radius of a toe, based on the hip joint. Additionally, we analyzed the joint space using the same method, and obtained the same result with the musculoskeletal leg robot. PCA for the A-A activity clarified that joint stiffness during human running was dominantly controlled by one pattern of muscle coordination and adjusted by another pattern. For the next step, we will investigate the correspondence relation between the muscle space and the joint space, and might be able to dynamically control the musculoskeletal robot by using the extracted muscle synergies.

References:

[1] N. Bernstein, "The coordination and regulation of movements," Oxford, Pergamon, 1967.
[2] G. Cappellini, Y. P. Ivanenko, R. E. Poppele, and F. Lacquaniti, "Motor Patterns in Human Walking and Running," J. Neurophysiol., Vol.95, No.6, pp. 3426-3437, 2006.
[3] Y. P. Ivanenko, R. E. Poppele, and F. Lacquaniti, "Five basic muscle activation patterns account for muscle activity during human locomotion," J. Physiol., Vol.556 (Pt.1), pp. 267-282, 2004.
[4] Y. P. Ivanenko, R. E. Poppele, and F. Lacquaniti, "Motor Control Programs and Walking," Neuroscientist, Vol.12, No.4, pp. 339-348, 2006.
[5] Y. P. Ivanenko, G. Cappellini, N. Dominici, R. E. Poppele, and F. Lacquaniti, "Modular Control of Limb Movements during Human Locomotion," J. Neurosci., Vol.27, No.41, pp. 11149-11161, 2007.
[6] H. Hirai, K. Matsui, T. Iimura, K. Mitsumori, and F. Miyazaki, "Modular Control of Limb Kinematics During Human Walking," Proc. of 2010 IEEE Int. Conf. Biomedical Robotics and Biomechatoronics (BioRob2010), pp. 716-721, 2010.
[7] D. A. Neumann, "Kinesiology of the Musculoskeletal System," Mosby, 2002.
[8] E. Criswell, "Cram's Introduction to Surface Electromyography Second Edition," Jones & Bartlett Pub., 2008.
[9] V. M. Zatsiorsky, "Kinetics of human motion," Human Kinetics, 1997.
[10] Human body properties database, http://riodb.ibase.aist.go.jp/dhbodydb/properties/s/index-e.html

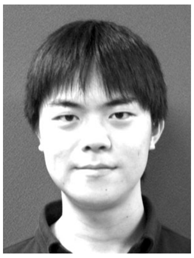

Name:
Taiki Iimura

Affiliation:
Master Course Student, Graduate School of Engineering Science, Osaka University

Address:
1-3 Machikaneyama-cho, Toyonaka, Osaka 560-8531, Japan

Brief Biographical History:
2010 Received the B.E. degree from Osaka University
2010- Master Course Student at Graduate School of Engineering Science, Osaka University

Main Works:
• T. Iimura, K. Inoue, H. T. T. Pham, H. Hirai, and F. Miyazaki, "A Preliminary Experiment for Transferring Human Motion to a Musculoskeletal Robot – Decomposition of Human Running based on Muscular Coordination –," In Proc. of the 2011 IEEE/RSJ Int. Conf. on Intelligent Robots and Systems (IROS2011), San Francisco, 2011.
• T. Iimura, K. Inoue, H. Hirai, and F. Miyazaki, "Decomposition and Combination of Motions based on Muscular Coordination during Human Running," In Proc. of 2010 SICE Conf. System Integration (SI2010), Miyagi, Japan, 2010.

Membership in Academic Societies:
• Institute of Electrical and Electronics Engineers (IEEE) (Student Member)
• The Society of Instrument and Control Engineers (SICE) (Student Member)
• The Japan Society of Mechanical Engineers (JSME) (Student Member)

Name:
Keita Inoue

Affiliation:
Master Course Student, Graduate School of Engineering Science, Osaka University

Address:
1-3 Machikaneyama-cho, Toyonaka, Osaka 560-8531, Japan

Brief Biographical History:
2010 Received the B.E. degree from Osaka University
2010- Master Course Student at Graduate School of Engineering Science, Osaka University

Main Works:
• K. Inoue, T. Iimura, H. Hirai, and F. Miyazaki, "Roles of PCs of Agonist-Antagonist Muscle Pairs Ratio in Human Walking," In Proc. of 2010 the Robotics Society of Japan Conf. (RSJ2010), Aichi, Japan, 2010.

Membership in Academic Societies:
• The Japan Society of Mechanical Engineers (JSME) (Student Member)
• The Robotics Society of Japan (RSJ) (Student Member)

Name:
Hang T. T. Pham

Affiliation:
Doctor Course Student, Graduate School of Engineering Science, Osaka University

Address:
1-3 Machikaneyama-cho, Toyonaka, Osaka 560-8531, Japan

Brief Biographical History:
2006 Received the B.E. degree from Hanoi University of Technology
2010 Received the M.E. degree from Graduate School of Engineering Science, Osaka University
2010- Doctor Course Student, Graduate School of Engineering Science, Osaka University

Main Works:
• H. T. T. Pham, R. Ueha, H. Hirai, and F. Miyazaki, "A Study on Dynamical Role Division in a Crank-Rotation Task from the Viewpoint of Kinetics and Muscle Activity Analysis," In Proc. of the 2010 IEEE/RSJ Int. Conf. on Intelligent Robots and Systems (IROS2010), Taipei, 2010.
• H. T. T. Pham, M. Kimura, H. Hirai, and F. Miyazaki, "Extraction and Implementation of Muscle Synergies in Hand-Force Control," In Proc. of the 2011 IEEE Int. Conf. on Robotics and Automation (ICRA2011), pp. 3658-3663, 2011.

Name:
Hiroaki Hirai

Affiliation:
Associate Professor, Graduate School of Engineering Science, Osaka University

Address:
1-3 Machikaneyama Town, Toyonaka, Osaka 560-8531, Japan

Brief Biographical History:
1999 Received the M.E. degree from Graduate School of Engineering Science, Osaka University
2004 Received the Ph.D. degree from Graduate School of Engineering Science, Osaka University
2004- Postdoctoral Fellow, Ritsumeikan University
2005- Assistant Professor, Osaka University
2010- Associate Professor, Osaka University

Main Works:
• H. Hirai and F. Miyazaki, "Dynamic Coordination Between Robots: The Self-organized Timing Selection in a Juggling-like Ball Passing Task," IEEE Trans. on Systems, Man, and Cybernetics PART B, Vol.36, No.4, pp. 738-754, 2006.

Membership in Academic Societies:
• Institute of Electrical and Electronics Engineers (IEEE)
• The Robotics Society of Japan (RSJ)
• The Society of Instrument and Control Engineers (SICE)
• The Institute of Systems, Control and Information Engineers (ISCIE)

Name:
Fumio Miyazaki

Affiliation:
Professor, Graduate School of Engineering Science, Osaka University

Address:
1-3 Machikaneyama-cho, Toyonaka, Osaka 560-8531, Japan

Brief Biographical History:
1977 Received the M.E. degree from Graduate School of Engineering Science, Osaka University
1979- Assistant Professor, Osaka University
1982 Received the Ph.D. degree from Graduate School of Engineering Science, Osaka University
1986- Associate Professor, Osaka University
1987-1988 Visiting Associate Professor, the University of California, Santa Barbara
1991- Professor, Osaka University
1995-1997 Visiting Professor, Institute of Space and Astronautical Science (ISAS)

Main Works:
• F. Miyazaki, M. Matsushima, and M. Takeuchi, "Learning to Dynamically Manipulate: A Table Tennis Robot Controls a Ball and Rallies with a Human Being," Advances in Robot Control, pp. 317-341, Springer, 2006.

Membership in Academic Societies:
• Institute of Electrical and Electronics Engineers (IEEE)
• The Robotics Society of Japan (RSJ)
• The Society of Instrument and Control Engineers (SICE)
• The Japan Society of Mechanical Engineers (JSME)
• The Institute of Systems, Control and Information Engineers (ISCIE)